HIV-specific CD8+ T-cell proliferative response 24 weeks after early antiretroviral therapy initiation predicts the subsequent reduction of the viral reservoir

Pien M. van Paassen[1,2 #], Alexander O. Pasternak[2,3 #], Dita C. Bolluyt[2,3,10], Karel A. van Dort[1,2], Ad C. van Nuenen[1,2], Irma Maurer[1,2], Brigitte Boeser-Nunnink[1,2], Ninée V.E.J. Buchholtz[4], Tokameh Mahmoudi[5], Cynthia Lungu[5], Reinout van Crevel[6], Casper Rokx[7], Jori Symons[4], Monique Nijhuis[4], Annelou van der Veen[10], Liffert Vogt[8,9], Michelle J. Klouwens[10], Jan M. Prins[10], Neeltje A. Kootstra[1,2 $], Godelieve J. de Bree[10 $]; on behalf of the Netherlands Cohort Study on Acute HIV Infection (NOVA) study team

[1]Department of Experimental Immunology, Amsterdam UMC, Amsterdam, The Netherlands; [2]Amsterdam Institute for Infection and Immunity, Amsterdam UMC, Amsterdam, The Netherlands; [3]Department of Medical Microbiology and Infection Prevention, Laboratory of Experimental Virology, Amsterdam UMC, Amsterdam, The Netherlands; [4]Department of Medical Microbiology, Translational Virology, University Medical Center Utrecht, the Netherlands; [5]Department of Biochemistry and Department of Pathology, Erasmus Medical Center, Rotterdam, The Netherlands; [6]Department of Internal Medicine and Radboud Center for Infectious Diseases, Radboud University Medical Center, Nijmegen, the Netherlands; [7]Department of Internal Medicine and Department of Medical Microbiology and Infectious Diseases, Erasmus University Medical Center, Rotterdam, The Netherlands; [8]Apheresis Unit, Dianet, location Amsterdam UMC, Amsterdam, The Netherlands; [9]Department of Internal Medicine, section Nephrology, Amsterdam UMC, location AMC, Amsterdam, The Netherlands; [10]Department of Internal Medicine, section Infectious Diseases, Amsterdam UMC, location AMC, Amsterdam, The Netherlands

[#]These authors contributed equally to this work and share the first authorship

[$]These authors also contributed equally to this work and share the last authorship

Corresponding author: Pien van Paassen, Meibergdreef 9, 1105 AZ Amsterdam, The Netherlands, phone: +31 6 42970500, email: p.vanpaassen@amsterdamumc.nl

CR received research grants for investigator initiated studies, and reimbursement for scientific advisory board participation and travel from Gilead Sciences and ViiV Healthcare. MN received consultancy fees from ViiV Healthcare. The other authors declare no conflicts of interest.

Abstract

Antiretroviral therapy (ART) initiated in the acute phase of HIV infection (AHI) results in a smaller viral reservoir. However, the impact of early HIV-specific T-cell responses on long-term reservoir dynamics is less well characterized. Therefore, we measured the size of the viral reservoir and functionality of HIV-specific CD8+ T-cell responses after the acute phase at 24 and 156 weeks after ART initiation in individuals who started treatment during AHI. A significant reduction in total and defective HIV DNA and a trend towards a reduction in intact HIV DNA were observed between 24 and 156 weeks. Functional CD8+ T-cell responses against HIV peptides Env, Gag, Nef, and Pol were maintained over three years after treatment initiation. The proliferative capacity of HIV-specific CD8+ T cells at 24 weeks of ART was predictive of the degree of reduction in total and defective HIV DNA between 24 and 156 weeks, suggesting HIV-specific CD8+ T-cells may at least partially drive the decline of the viral reservoir. Therefore, enforcing HIV-specific immune responses as early as possible after diagnosis of AHI should be a central focus of HIV cure strategies.

Introduction

Current treatment of HIV infection with antiretroviral therapy (ART) successfully suppresses viral replication, halts and reverses disease progression, and gives people with HIV (PWH) a near-normal life expectancy (1). However, ART does not clear HIV infection and must be taken lifelong. This is due to the persistence of the viral reservoir, which remains the central barrier to achieving HIV eradication or long-term remission. The long-term persistence of viral reservoir is the result of HIV integration into the host genome: the integrated provirus persists for the lifespan of the infected cell, and if this cell divides, the provirus is passed on to its progeny. As soon as ART is interrupted, the reservoir will almost inevitably fuel prompt viral rebound (2-4).

During the early stages of HIV infection, also referred to as acute HIV infection (AHI), active viral replication supports rapid seeding of the viral reservoir within lymph nodes and other tissues like the spleen and gut-associated lymphoid tissue (5, 6). HIV reservoir is established extremely early after infection: a study in non-human primates (NHP) has shown that this happens even before detectable viremia (7). The early immune response during AHI is critical in shaping the course of infection and the size of the viral reservoir (7). Along with rising viral levels, cytokine and chemokine levels increase, which recruit and activate innate immune cells (8, 9). These regulate the subsequent adaptive immune response (10). HIV-specific CD8+ cytotoxic T lymphocytes (CTLs) appear 2-3 weeks after infection and are thought to contribute to the initial decline in plasma viremia before ART is initiated (11, 12). Conversely, active viral replication shapes the magnitude and diversity of HIV-specific CD8+ T-cells, especially during this early stage of infection (13). Moreover, CD8+ T-cells exert immune pressure by recognizing and killing infected cells that present HIV-derived peptides via HLA class I molecules. Indeed, individuals expressing protective HLA alleles such as HLA-B57 and HLA-B27 tend to mount more effective CD8+ T-cell responses and exhibit lower viral set points (14).

In addition to limiting active viral replication, CD8+ T-cells may also influence the composition and dynamics of the viral reservoir. Although ART effectively halts new rounds of infection, it does not eliminate long-lived infected cells harboring intact proviral DNA. Emerging evidence suggests that CD8+ T-cell pressure can shape which proviruses persist by selectively eliminating infected cells that express viral antigens during latency reversal or low-level transcription (15, 16).

The importance of the host CD8+ T-cell response in controlling virological outcomes is supported by many studies. For instance, strong HIV-specific CD8+ T-cell responses have been shown to control HIV replication without ART in human elite (17-20) and post-treatment controllers (PTC) (21, 22), and to control SIV replication in non-human primates (NHP) (23-25). The quality of the CD8+ T-cell response is defined by its breadth, magnitude, polyfunctionality, and cytolytic capacity, and has been associated with better viral control and slower disease progression (26-28). However, in the majority of PWH, CD8+ T-cell dysfunctionality is already observed shortly after peak viremia during AHI, which could potentially be prevented if ART is initiated prior to this occurring (13, 29). Indeed, effective HIV-specific CD8+ T-cell responses were observed in people treated during AHI and the magnitude of this response correlated with the transcriptional activity of the virus (30). ART initiation during AHI also resulted in a smaller viral reservoir size by limiting viral replication and seeding of the reservoir compared to treatment initiation during chronic infection (CHI) (12, 13, 31-35). Moreover, early ART initiation enhances restoration of the immune system (35, 36). The importance of ART initiation during AHI is underscored by the fact that early treated individuals have a higher chance of achieving at least temporary viral control after stopping ART (37).

Currently, it is unknown whether early ART can preserve functionality of HIV-specific CD8+ T-cell responses and how these relate to the viral reservoir long-term. In this study, we aimed to characterize these dynamics in participants of the Netherlands Cohort Study on Acute HIV Infection (NOVA study), who initiated ART immediately after diagnosis of AHI and were followed for over three years. We found evidence that the early immune response shapes aspects of the viral reservoir when ART is initiated during AHI.

Results

Cohort description

This study included 22 participants of the NOVA cohort who initiated ART immediately (median 1 day, IQR 0-2) after diagnosis during AHI. We selected those participants for whom leukapheresis samples at either 24 weeks and/or 156 weeks post ART initiation were available. Samples from both time points were available from twelve of 22 participants, resulting in a total of 34 samples. Baseline characteristics are provided in Table 1. The median age at time of inclusion was 38 years (IQR 28-48), all participants were male and two-third of participants had a subtype B HIV infection. At diagnosis, participants had a median plasma viral load (pVL) of 0.4×10^6 copies/mL (Suppl. Fig. 2A). Two participants had a detectable pVL of 200 and 100 copies/mL (Participant X) and 74 and 98 copies/mL (Participant Y), at 24 and 156 weeks respectively (Suppl. Fig. 2A).

CD4+ T-cell counts at 24 weeks and 156 weeks were comparable, with a median of 610 (IQR 520-725) and 695 (IQR 623-838) cells/mm^3 respectively (Suppl. Fig. 2B; p=0.13), as were the CD8+ T-cell counts (median 680 (IQR 485-840) at 24 weeks and 730 (IQR 520-1005)

cells/mm^3 at 156 weeks (p=0.41). The CD4/CD8 ratio increased significantly between baseline and 24 weeks (Suppl. Fig. 2C; p<0.01), but was comparable between 24 and 156 weeks.

Longitudinal reduction of total and relative increase in transcription-competent viral reservoir

First, we determined the HIV reservoir size at 24 and 156 weeks by measuring total, intact, and defective HIV DNA in PBMCs. Intact and defective proviruses were measured by intact proviral DNA assay (38). Intact (*psi*+ *env*+) proviruses were detected in 33 of 34 samples, while defective proviruses (either 3' defective [*psi*+ *env*-] or 5' defective [*psi*- *env*+]) were detectable in all samples. A number of studies have shown that viral latency does not preclude viral transcription (39). Therefore, we also quantified cell-associated unspliced (US) HIV RNA as a measure of transcriptionally active reservoir at 24 and 156 weeks. To better understand the relationships between these different measures of the viral reservoir, Spearman correlation analysis was conducted at 24 and 156 weeks. At both time points, strong positive correlations were observed between the levels of total HIV DNA, 3' defective HIV DNA, and US RNA (Fig. 1). At 24 weeks but not at 156 weeks, nonsignificant trends towards positive correlations of intact HIV DNA with total DNA and US RNA were observed (p=0.09 and p=0.10, respectively), and both total DNA and US RNA did not correlate with 5' defective DNA at any time point (Fig. 1).

At the 24-week time point, replicating virus could be isolated by Quantitative Viral Outgrowth Assay (QVOA) from CD4+ T-cells of six participants, one of whom had a detectable plasma viral load at that time point (Participant Y, 74 copies/mL). For four out of these six participants, 156-week samples were available, but replication-competent virus could not be retrieved from any of them. We compared the intact HIV DNA levels at the 24-week timepoint between the

six participants, from whom we were able to isolate replicating virus, and the fourteen participants, from whom we could not. Participants with positive QVOA had significantly higher intact HIV DNA levels than those with negative QVOA (p=0.029, Mann-Whitney test; Suppl. Fig. 3). Five of six participants with positive QVOA had intact DNA levels above 100 copies/10^6 PBMC, while thirteen of fourteen participants with negative QVOA had intact HIV DNA below 100 copies/10^6 PBMC (p=0.0022, Fisher's exact test). These findings indicate that recovery of replication-competent virus by QVOA is more likely in individuals with higher levels of intact HIV DNA in IPDA, reaffirming a link between the two measurements.

Next, we included participants with available samples from both time points (n=12) in a comparative analysis of the reservoir measures between 24 and 156 weeks ART (Fig. 2). Significant reductions in levels of total (p=0.02), 3' defective (p<0.01), and total defective (p<0.01) HIV DNA were observed from 24 to 156 weeks. Furthermore, we noted a trend towards a reduction in intact HIV DNA level from 24 to 156 weeks (p=0.11). No significant differences in 5' defective HIV DNA as well as US RNA levels (p=0.23 for both comparisons) were observed between 24 and 156 weeks. However, relative HIV transcription level per provirus, calculated as US RNA/total HIV DNA (US/TD) ratio, significantly increased between 24 and 156 weeks (p=0.03), indicating a relative increase in transcriptional activity of the reservoir over time.

Comparable frequency and function of the HIV-specific CD8+ T-cell response at 24 and 156 weeks

General phenotyping of CD4+ (Suppl. Fig. 4A) and CD8+ (Suppl. Fig. 4B) T-cells showed no difference in frequencies of naïve, memory or effector CD4+ and CD8+ T-cells between 24 and 156 weeks. Moreover, CD8+ T-cell activation levels were low (<10%) and remained stable

over time (Suppl. Fig. 4B). Next, HIV-specific CD8+ T-cell numbers and functionality at 24 and 156 weeks post ART initiation were analyzed. A subgroup of participants (n=9), positive for HLA-type HLA-A*2, HLA-B*7, or both, showed similar frequencies of HIV-specific dextramer positive CD8+ T-cells at 24 and 156 weeks (median frequency 0.066% (IQR 0.031-0.11) at 24 weeks and 0.055% (IQR 0.052-0.11) at 156 weeks (Suppl. Fig. 5A; p=0.48). The phenotype of HIV-dextramer specific CD8+ T-cells showed no difference in expression of exhaustion markers (upregulation of PD-1, CTLA-4, and CD160 expression; loss of CD28 expression) between the two time points (Suppl. Fig. 5B).

HIV-specific CD8+ T cell functionality was assessed through stimulation with HIV Env, Gag, Nef and Pol peptide pools. The readout of these stimulation was the interferon gamma release assay (IGRA), activation-induced marker (AIM) assay and cell proliferation (precursor frequency and proliferated cells). IFN-γ responses to Env, Gag, Nef and Pol were observed in 3, 8, 2 and 1 participant(s), respectively, at 24 weeks and 1, 7, 2 and 1 participant(s), respectively, at 156 weeks (data not shown). The AIM assay showed a similar broad HIV-specific T-cell response to at least three different viral proteins in the majority of individuals at both time points (data not shown). The magnitude of the T-cell response, by combining the frequencies of reactive CD8+ T-cells to all viral proteins (Env, Gag, Nef, Pol) tested, showed no statistically significant differences (Suppl. Fig. 6B) over time. Similarly, a broad HIV-specific CD8+ T-cell proliferative response to at least three different viral proteins was observed in the majority of individuals at both time points. At 24 weeks, 6/11 individuals had a response to Env, 10/11 to Gag, 5/11 to Nef, and 4/11 to Pol. At 156 weeks, 8/11 to Env, 10/11 to Gag, 8/11 to Nef and 9/11 to Pol, with no significant differences in precursor frequencies and proliferative capacity between week 24 and week 156 (Suppl. Fig. 6C&D).

Magnitude of proliferative HIV-specific CD8+ T-cell response predicts the reduction of the viral reservoir

Next, we performed a Spearman correlation analysis between these responses and viral reservoir measurements. The frequencies of HIV-specific dextramer positive CD8+ T-cells did not correlate with any of the reservoir measurements at 24 or 156 weeks (Suppl. Fig. 7). Also, neither HIV-specific CD8+ T-cell functionality as determined by IGRA nor proportion of HIV-reactive (AIM) CD8+ T-cells showed any correlation with the viral reservoir at 24 weeks (Fig. 3). However, at this time point, HIV-specific CD8+ T-cell proliferative response positively correlated with the levels of total and total defective HIV DNA (*rho*=0.62, p=0.037 and *rho*=0.70, p=0.014, respectively). At 156 weeks, however, these correlations were no longer observed (Fig. 3).

To determine whether any immunological parameters measured at 24 weeks ART were predictive for the subsequent change in the viral reservoir size, we fitted statistical models, in which we included age and ART regimen, in addition to three different measures of HIV-specific CD8+ T-cell responses, as explanatory variables, and changes in total, intact, and total defective HIV DNA between 24 and 156 weeks ART as dependent variables (Table 2). As the vast majority of participants were treated with integrase strand transfer inhibitor-based ART, we only included the nucleotide reverse transcriptase inhibitor backbone as ART regimen in the models. Neither age nor ART regimen nor IFN-γ release nor CD8+ T-cell reactivity was predictive for the subsequent change in the reservoir size. However, CD8+ T-cell proliferative response at 24 weeks was predictive for the degree of reduction in total and total defective HIV DNA (p=0.014 and p=0.0017, respectively) (Table 2). This suggests that the early presence of HIV-specific CD8+ T-cells with an enhanced proliferative capacity in response to HIV plays a role in the reduction of the viral reservoir over the course of 2.5 years.

Discussion

In this study, we investigated the longitudinal dynamics of the HIV reservoir and host immunological responses in people immediately treated with ART during AHI. We found a reduction in the viral reservoir, as evidenced by the significant reduction in total- and defective HIV DNA and the trend towards a reduction in intact HIV DNA, between 24 and 156 weeks on ART. Strikingly, this reduction in total- and defective HIV DNA levels over time was predicted by HIV-specific proliferative CD8+ T-cell responses against HIV peptides Env, Gag, Nef and Pol at 24 weeks. We also observed that HIV-specific CD8+ T-cell responses were maintained over three years after treatment initiation.

We observed that the defective HIV DNA levels decreased significantly between 24 and 156 weeks of ART. This is different from studies in CHI, where no significant decrease during the first 7 years of ART (40, 41), or only a significant decrease during the first 8 weeks on ART, but not in the 8 years thereafter, was observed (42). The integrated, but defective proviruses do not produce replicating virus but can be transcriptionally and translationally competent and are therefore thought to play a substantial role in ongoing immune activation (43). Indeed, it was shown that these defective proviruses are capable of producing viral RNA transcripts and proteins both in vivo and in vitro (44, 45). In our cohort, at 24 weeks US RNA correlated with defective HIV DNA levels but not with intact HIV DNA. This suggests that the US RNA transcripts are mainly produced from defective proviruses. Moreover, the correlation between the HIV-specific CD8+ T-cell response and defective HIV DNA levels suggest detection by the immune system, leading to decay and shaping of the proviral landscape. This is in line with a study showing that CTLs indeed target defective proviruses (46). Importantly, reservoir decay patterns are not only influenced by HIV-specific immune responses, but are also known to be

associated with other factors. A recent study found that there was a faster decay of intact and defective HIV DNA when ART was initiated earlier, initial CD4+ T-cell counts were higher and pre-ART pVL was lower (47). Indeed, a recent study investigated reservoir dynamics in people that initiated ART during hyperacute HIV-1 in subtype C infection and found that early ART was associated with reduced phylogenetic diversity and rapid decay of intact proviruses (48). In fact, no intact provirus could be detected after 1 year of ART (reduction of 51% per month), while a decline in defective provirus was observed (reduction of 35% per month) (48). In our cohort, we observed a significant decrease in total- and defective HIV DNA load between 24 weeks and 3 years, while the decline of intact HIV DNA was less pronounced. This discrepancy could possibly be explained by the time period after AHI that was analyzed, as in that study decay of intact HIV DNA was observed in the first six months of treatment (48), while we determined the reduction between weeks 24 and 156. Similarly, in another study, a comparable biphasic decay was found in total (half-life 12.6 weeks) and integrated (half-life 9.3 weeks) HIV DNA in AHI, but total HIV DNA continued to decline in the second decay phase (49). Recent mathematical modelling of reservoir decay in AHI between 0-24 weeks after ART initiation showed a biphasic decay for both intact and defective DNA (47). Intact DNA showed a rapid initial $t_{1/2}$ during the first 5 weeks of ART followed by a slower decay with a $t_{1/2}$ of around 15 weeks. Defective DNA showed an even significantly larger decrease in the first phase than intact DNA, followed by a slower decay (47). The lack of significant reduction of intact HIV DNA in our study may also be explained by ongoing immune-mediated selection of integrated intact proviral DNA in repressive and heterochromatin locations, eventually resulting in a shift towards a state of “deep latency”, which has been suggested previously (50) and also seen in people who naturally control HIV (elite controllers) (51, 52). This way, these intact proviruses are not expressed and hence not eliminated by the immune system, which could explain why we do not see a significant reduction. Interestingly, we could only retrieve

replication-competent virus from six out of twenty participants at week 24 and from none at week 156, indeed suggesting selection for integrated intact proviruses that are not rebound-competent upon reactivation.

The relationship between HIV reservoir reduction and HIV-specific CD8+ T-cell responses has been recently investigated by Takata et al. in a study that included two Thai cohorts with participants starting ART during AHI and CHI, respectively (30). In CHI, they found a similar reduction in HIV reservoir over two years on ART, however CD8+ T-cell responses also declined. In AHI, overall the reservoir was lower, and the frequency of reactive CD8+ T-cells 96 weeks after ART initiation was comparable to the frequency in CHI. Importantly, a larger HIV reservoir size hampered differentiation into functional HIV-specific CD8+ T-cells (30). In our study, we did not see a change in number of HIV-specific CD8+ T-cell responses over time and even more so, we found a preserved functionality up to three years after ART start. In contrast to the Takata study (30), in our cohort we did not observe a significant correlation between cell-associated HIV US RNA and HIV-specific CD8+ T-cell responses. Further studies should investigate whether viral transcription drives the CD8+ T-cell response. Interestingly, we observed a significant increase in the US RNA/total HIV DNA ratio between 24 and 156 weeks, suggesting a paradoxical shift towards a more transcriptionally active reservoir despite an overall reduction in the reservoir size. The mechanism behind this effect is unclear but may involve preferential survival of transcriptionally active proviral clones with time on ART.

The use of different readouts may explain at least some of the differences observed between studies. The study by Takata et al. reported a decline in functional CD8+ T-cell responses after two years of ART based on a combined AIM/intracellular staining assay (ICS) and using a different activation marker (4-1BB) (30). In our cohort, we used both the AIM and proliferation

assay to determine that HIV-specific CD8+ T-cell responses were maintained. Interestingly, relations similar to our study between the HIV reservoir size decline and HIV-specific CD8+ T-cell responses were reported (30). However, Takata et al. showed loss of the association when total HIV DNA was used as a reservoir marker, whereas we report here a predictive value of HIV-specific CD8+ T-cell responses for the reduction in both total and defective HIV DNA.

There are some limitations to this study. First, our cohort consists of only males, who are mostly of European descent. Therefore, our findings might not apply to people of different ethnicities or females. It is known that host genetic factors (related to different ethnicities or sex at birth) influence immune responses and viral reservoir characteristics (53). Second, not all participants underwent leukapheresis at the 156 week time point due to personal or logistic (COVID-19 pandemic) reasons and therefore we had a small longitudinal sample size, that included participants ranging from Fiebig II-VI. Therefore we could not assess the role of the Fiebig stage at ART initiation. A strength of our study is the long-term sampling, which allowed us to assess the reservoir decay and host immune responses years after ART initiation. Previously mentioned studies into reservoir decay have mainly reported on the first year after treatment was started (47, 48, 54).

In summary, our study shows that between 24 weeks and 3 years of ART, total- and defective HIV DNA reduced significantly and that this reduction is predicted by the magnitude of HIV-specific CD8+ T-cell responses at 24 weeks. This suggests that HIV-specific CD8+ T-cells may at least partially drive the decline of the viral reservoir. Our study has several implications. First, it confirms the complexity of host-virus interplay, as we show that defective HIV DNA decreased stronger than intact HIV DNA, and defective, but not intact, HIV DNA correlated with US RNA and the functionality of the HIV-specific CD8+ T cell response. However, the reduction of defective HIV DNA did not result in a decreased HIV transcriptional activity over

time. This could be the result of selection for cells that harbor transcriptionally active proviruses that circumvent immune surveillance through for instance upregulation of immune inhibitory molecules like PD-1, CTLA-4 and TIGIT, downregulation of HLA class I molecules, or the emergence of viral escape mutations. Second, our study shows that even in acute treated HIV infection, the reservoir is readily detectable despite immediate ART. We believe our study underscores that in line with what was shown in natural HIV control, an (early) functional CD8+ T-cell response is shaping the viral reservoir during ART and that enhancing host immune responses should be a focus for interventions aimed at a functional HIV cure.

Author contributions

Conceived and designed the experiments: PvP, AOP, JMP, NAK, GJdB. Performed the experiments and analyzed the data: PvP, AOP, KAvD, ACvN, IM, BBN, NVEJB, JMP, NAK, GJdB. Contributed to reagents, materials, and analysis tools: PvP, AOP, KAvD, ACvN, IM, BBN, NVEJB, TM, CL, CR, JS, MN, LV, MJK, JMP, NAK, GJdB. Wrote the paper: JP, NK, AOP, and PvP. Reviewed and edited manuscript: PvP, AOP, KAvD, ACvN, IM, BBN, NVEJB, TM, CL, CR, JS, MN, LV, MJK, JMP, NAK, GJdB.

Acknowledgments

We would kindly like to thank all participants of the NOVA cohort study. We would also like to thank all medical doctors, lab personnel and research nurses, including A. Weijsenfeld and F. Pijnappel (Amsterdam University Medical Center), A. Karisli (Erasmus University Medical Center) and K. Grintjes (Radboud University Medical Center). This research was funded by

Gilead Sciences, funding number CO-NL-985-6195, and Aidsfonds, funding number P-60803. AOP acknowledges grant support from amfAR, The Foundation for AIDS Research (grant no. 1110680–77-RPRL), and from Partnership NWO-Dutch AIDS Fonds ‘HIV cure for everyone’ (grant no. KICH2.V4P.AF23.001).

Methods

Sex as a biological variable. The NOVA study is open for inclusion to both males and females; however, in the current study only samples from male participants were available. This reflects the epidemiology of acute/early HIV infections in the Netherlands, which concerns mostly males. We do believe more females should be included in this research to be able to translate the findings to the entire population that is currently living with HIV.

Study approval. The NOVA cohort is a multicenter, observational, prospective cohort that was initiated in 2015 and includes participants diagnosed with an acute/early HIV infection (AHI) (55). The study was approved by the Medical Ethics Committee of the Amsterdam UMC (NL51613.018.14) and all study participants gave written informed consent.

Study design. The study design of the NOVA study, including treatment regimen and follow-up visits, has been described elsewhere (55). In short, people were included if they were 18 years or older and were diagnosed during AHI as defined by Fiebig stage I-IV. In case of a positive Western blot, participants could only be included if they had a documented negative HIV screening test <6 months before inclusion. After diagnosis, participants were referred to an HIV treatment center and started a four-drug regimen of emtricitabine/tenofovir 200/245 mg (FTC/TDF), dolutegravir 50 mg (DTG), darunavir 800 mg and ritonavir 100 mg (DRV/r) as soon as possible (preferably within 24 hours). After four weeks, when baseline genotyping and viral mutations conferring possible drug resistance were known, DRV/r was discontinued. Participants could enroll in three groups based on the preparedness of individuals to undergo extensive sampling (Suppl. Fig. 1). Participants that accepted immediate treatment and follow-up but declined additional blood and tissue sampling were included in study group 1, of which only routine clinical care plasma viral load (pVL) and CD4 count measurements were collected. For group 2 and 3, PBMC and semen were collected at study visits and cryopreserved, in group

3 in addition GALT, lymph node biopsies and CSF were collected. In both groups leukapheresis was performed at weeks 24 and 156. The participants selected for the current analysis were in care at Amsterdam University Medical Center, Erasmus University Medical Center or Radboud University Medical Center. Apart from pVL and CD4/CD8 measurements, all virological and immunological assessments were performed centrally at the Amsterdam University Medical Center.

Viral load quantification and HIV subtyping. Viral load (HIV RNA) was measured in plasma using a sensitive HIV RNA assay. The assays that were used were m2000rt HIV RNA (Abbott) with a lower limit of quantification (LLOQ) of 40 copies/mL from 2015-2021, Alinity m HIV-1 Assay (Abbott) with a LLOQ of 20 copies/mL from 2021 onwards (Amsterdam University Medical Center), COBAS AmpliPrep/COBAS TaqMan HIV-1 test (Roche Diagnostics), LLOQ 20 copies/mL and Aptima HIV-1 Quant Dx Assay (Hologic), LLOQ 30 copies/mL (Erasmus Medical Center), and Xpert HIV-1 assay (Cepheid) with a LLOQ of 40 copies/mL (Radboud University Medical Center). HIV subtypes were determined using Neighbor joining analysis to create phylogenetic trees. Reference sequences from the major HIV-1 subtypes were obtained from the NCBI database and the distance between sequences was calculated using the Kimura-2 parameter model.

Quantification of total HIV DNA and cell-associated unspliced HIV RNA. Total HIV DNA and cell-associated unspliced (US) HIV RNA were quantified by semi nested qPCR according to the principles described previously (56). In brief, total nucleic acids were extracted from PBMCs using Boom isolation method (57). Extracted cellular RNA was treated with DNase (DNA-free kit; ThermoFisher Scientific) to remove genomic DNA that could interfere with the quantitation and reverse transcribed into cDNA using random primers and SuperScript III reverse transcriptase (all from ThermoFisher Scientific). To quantify cell-associated US HIV RNA or total HIV DNA, this cDNA, or DNA extracted from PBMCs, respectively, was pre-

amplified using primer pair Ψ_F (38) and HIV-FOR (58). The product of this PCR was used as template for a semi-nested qPCR with the Ψ primer/probe combination (59). HIV DNA or RNA copy numbers were determined using a 7-point standard curve with a linear range of more than 5 orders of magnitude that was included in every qPCR run and normalized to the total cellular DNA (by measurement of β-actin DNA) or RNA (by measurement of 18S ribosomal RNA) inputs, respectively, as described previously (60). Non-template control wells were included in every qPCR run and were consistently negative. Total HIV DNA and US RNA were detectable in 88.2% and 73.5% of the samples, respectively. Undetectable measurements of US RNA or total DNA were assigned to the values corresponding to 50% of the corresponding assay detection limits. The detection limits depended on the amounts of the normalizer (input cellular DNA or RNA) and therefore differed among samples. HIV transcription levels per provirus (US RNA/total DNA ratios) were calculated taking into account that 10^6 PBMCs contain 1 μg of total RNA (61).

Quantification of intact and defective HIV DNA. Intact and defective HIV DNA was quantified by the intact proviral DNA assay (IPDA) (38). In brief, genomic DNA was isolated from PBMCs using Puregene Cell Kit (QIAGEN Benelux B.V.) according to the manufacturer's instructions and digested with *Bgl*I restriction enzyme (ThermoFisher Scientific) as described previously (62). Notably, only a small minority (<8%) of HIV clade B sequences contain *Bgl*I recognition sites between Ψ and env amplicons, therefore *Bgl*I digestion is not expected to substantially influence the IPDA output, while improving the assay sensitivity by increasing the genomic DNA input into a droplet digital PCR (ddPCR) reaction (62). After desalting by ethanol precipitation, genomic DNA was subjected to two separate multiplex ddPCR assays: one targeting HIV Ψ and *env* regions using primers and probes described previously, including the unlabeled *env* competitor probe to exclude hypermutated sequences (38), and one targeting the cellular *RPP30* gene, which was measured to correct for DNA

shearing and to normalize the intact HIV DNA to the cellular input. The *RPP30* assay amplified two regions, with amplicons located at exactly the same distance from each other as HIV Ψ and *env* amplicons. The first region was amplified using a forward primer 5'-AGATTTGGACCTGCGAGCG-3', a reverse primer 5'-GAGCGGCTGTCTCCACAAGT-3', and a fluorescent probe 5'-FAM-TTCTGACCTGAAGGCTCTGCGCG-BHQ1-3' (63). The second region was amplified using a forward primer 5'-AGAGAGCAACTTCTTCAAGGG-3', a reverse primer 5'-TCATCTACAAAGTCAGAACATCAGA-3', and a fluorescent probe 5'-HEX-CCCGGCTCTATGATGTTGTTGCAGT-BHQ1-3'. The ddPCR conditions were as described previously (38) with some minor amendments: we used 46 cycles of denaturation/annealing/extension and the annealing/extension temperature was 60°C. Intact HIV DNA was detectable in 97.0%, 3' defective HIV DNA in 76.5%, and 5' defective HIV DNA in 100% of the samples. QuantaSoft (version 1.7.4) was used for the data analysis. Positive and negative droplets were discriminated by manual thresholding.

Quantitative Viral Outgrowth Assay. Isolation of replication-competent virus was performed using CD4+ T-cell isolated PBMCs as described previously (64). PBMCs were thawed and CD4+ T-cells were isolated by negative selection using MACS Microbeads (Miltenyi Biotec, Bergisch Gladbach, Germany). A median of 20.5×10^6 CD4+ T-cells (IQR 12.5-39) per sample were used for the quantitative viral outgrowth assay (QVOA). For the QVOA, CD4+ T-cells were prestimulated for 48 hours by anti-CD3 (immobilized) (1XE) and anti-CD28 (15E8, 3 mg/ml) in Iscove's modified Dulbecco's medium (IMDM) supplemented with 10% (v/v) heat inactivated fetal calf serum (FCS), penicillin (100 U/ml), streptomycin (100 µg/ml), in a humidified 10% CO2 incubator at 37 °C. Subsequently, the CD4+ T-cells were co-cultured with 2-day PHA-stimulated donor PBMC in IMDM supplemented with 10% (v/v) heat inactivated FCS, penicillin (100 U/ml), streptomycin (100 µg/ml) and IL-2 (20 U/ml; Chiron Benelux). Every 7-days, fresh PHA-stimulated donor PBMC were added to propagate the

culture. Culture supernatants were regularly analyzed for viral replication using an in-house p24 antigen enzyme-linked immunosorbent assay (ELISA) (64).

Lymphocyte count determination. CD4+ and CD8+ T-cell counts were determined using cytometry at the study sites.

HLA typing. HLA genotyping was performed at the Department of Immunogenetics (Sanquin) by the PCR using sequence-based typing (SBT) method (GenDx Products, Utrecht, the Netherlands) and real-time (RT)- PCR (Thermofisher, West Hills, California, USA).

Immune phenotyping of T cells. PBMCs were used for immune phenotyping of CD8+ T cells. T-cell activation was defined as the proportion of cells positive for CD38 and HLA-DR; naïve T-cells as the proportion of CD45RA and CD27 positive cells, memory T-cells as proportion of CD45RA negative and CD27 positive cells and effector as proportion of CD45RA negative and CD27 negative cells. T-cell senescence was defined as CD27 and CD28 double negative cells. The following antibodies were used for staining: monoclonal antibody detecting CD3 (V500), CD4 (APC-H7), CCR7 (BV786)) from BD Biosciences (San Jose, USA); CD8 (Pacific Blue), CD45RA (BV605), CTLA4 (BV711), CD160 (PE-Cy7), CD28 (AF700) from BioLegend; and PD1 (PE) from eBioscience (San Diego, USA), HLA-DR (FITC), CD38 (PE), CD27 (APCeFluor 780), CD28 (PerCP Cy5.5), CD4+ (PE-Cy7), CD57 (APC)from BD Biosciences (San Jose, USA). The proportion of HIV-specific CD8+ T-cells was determined using APC-labeled MHC class I dextramers (Immudex, Virum, Denmark) carrying HLA-A*0201 SLYNTVATLY and HLA-B*0702 GPGHKARVL molecules in combination with CD3 (V500) and CD4 (APC-H7) from BD and CD8 (Pacific Blue) from BioLegend.

Fluorescence was measured on the FACS Canto II (BD Biosciences). The fractions of cells expressing a marker alone or in combination or the mean fluorescence intensity (MFI) were determined using FlowJo 7.6 (TreeStar, Ashland, Oregon).

Functional HIV cellular immune responses. An IFN-γ release assay was performed to evaluate the immune response upon HIV-peptide pool stimulation. A total of $0.5x10^6$ PBMCs were stimulated with HIV consensus B Env, Gag, Nef and Pol peptide pools (2 µg/ml, NIH AIDS Reagent Program) or cultured in medium alone as a control. After 1 day, culture supernatants were harvested and IFN-γ released by the cells was determined by human IFN-γ DuoSet ELISA (R&D Systems, Minneapolis, MN, USA).

The activation-induced marker (AIM) assay was performed to assess the frequency of reactive CD8+ T-cells. Therefore, PBMCs were stimulated for 6 hours with HIV peptide pools (Env, Gag, Nef and Pol) and then stained for flow cytometry. Reactive T-cells were determined by co-expression of CD137 (APC-H7/APC-Fire750) and CD69 (PE-Cy7) within the CD4+ and CD8+ T-cell populations, respectively. Fluorescence was measured on the FACS Canto II fluorescence-activated cell sorter (BD Biosciences). Marker expression levels were analyzed using FlowJo version 10.8.1 (TreeStar, Ashland, OR, USA).

Proliferation of CD8+ T-cells upon antigen stimulation was assessed through the use of the CellTrace™ VioleT-cell Proliferation kit (ThermoFisher). Cells were stained with CellTrace Violet according to manufacturer's protocol (0,5 uM final concentration) and flow cytometry analysis was used to determine that all the cells were labeled with Cell Trace Violet. Subsequently, the cells were stimulated with an HIV consensus B Gag, Env, Pol and Nef peptide pool (2ug/ml final concentration, NIH AIDS Reagent Program). An unstimulated control and positive controls using a peptide pool of CMVpp65 (2ug/ml final concentration, NIH AIDS Reagent Program) or α-CD3 in combination with α-CD28 were included. After 7 days cells were stained with FITC CD3, PerCP-Cy5.5 CD4+ (BD bioscience) and APC CD8+ (BioLegend) for 30 minutes at 4°C. After fixation of the cells with CellFIX (BD) samples were analyzed on the BD FACSCanto™ II to assess the proliferation of CD8+ T-cells under the different conditions. The proportion of proliferating cells was determined using FlowJo V10

(FlowJo). The precursor frequency is calculated as follows: per generation the amount of CD8+ T-cells that proliferated were calculated (number of cells * $2^{(generation)}$); the precursor frequency is the total number of CD8+ T-cells that proliferated per 100 CD8+ T-cells (total CD8+ T cells).

Statistical analysis. Reservoir measurements and T-cell responses were compared between 24 weeks and 156 weeks of ART using paired non-parametric Wilcoxon signed rank tests. Strength of correlations between different reservoir measures and between reservoir measured and T-cell responses was tested using non-parametric Spearman correlation analyses with Benjamini-Hochberg corrections for multiple comparisons (false discovery rate, 0.25). Intact proviral DNA levels were compared between participants with positive vs. negative QVOA using Mann-Whitney test. Proportions of participants with intact proviral DNA higher than 100 copies/10^6 PBMC were compared between those with positive vs. negative QVOA using Fisher's exact test. Predictive value of variables measured at 24 weeks ART for the changes in HIV-1 reservoir measures between 24 and 156 weeks of ART was modeled using generalized linear models (GLM). GLM were fitted on rank-transformed dependent variables and results of type III tests are reported. All tests were two-sided. P values <0.05 were considered statistically significant.

Data availability. All data from this study is available upon request to PvP (p.vanpaassen@amsterdamumc.nl).

References

1. Survival of HIV-positive patients starting antiretroviral therapy between 1996 and 2013: a collaborative analysis of cohort studies. Lancet HIV. 2017;4(8):e349-e56.
2. Chun TW, Davey RT, Jr., Engel D, Lane HC, Fauci AS. Re-emergence of HIV after stopping therapy. Nature. 1999;401(6756):874-5.
3. Davey RT, Jr., Bhat N, Yoder C, Chun TW, Metcalf JA, Dewar R, et al. HIV-1 and T cell dynamics after interruption of highly active antiretroviral therapy (HAART) in patients with a history of sustained viral suppression. Proc Natl Acad Sci U S A. 1999;96(26):15109-14.
4. Rothenberger MK, Keele BF, Wietgrefe SW, Fletcher CV, Beilman GJ, Chipman JG, et al. Large number of rebounding/founder HIV variants emerge from multifocal infection in lymphatic tissues after treatment interruption. Proc Natl Acad Sci U S A. 2015;112(10):E1126-34.
5. Daar ES, Moudgil T, Meyer RD, Ho DD. Transient high levels of viremia in patients with primary human immunodeficiency virus type 1 infection. N Engl J Med. 1991;324(14):961-4.
6. Pierson T, McArthur J, Siliciano RF. Reservoirs for HIV-1: mechanisms for viral persistence in the presence of antiviral immune responses and antiretroviral therapy. Annu Rev Immunol. 2000;18:665-708.
7. Whitney JB, Hill AL, Sanisetty S, Penaloza-MacMaster P, Liu J, Shetty M, et al. Rapid seeding of the viral reservoir prior to SIV viraemia in rhesus monkeys. Nature. 2014;512(7512):74-7.
8. Stacey Andrea R, Norris Philip J, Qin L, Haygreen Elizabeth A, Taylor E, Heitman J, et al. Induction of a Striking Systemic Cytokine Cascade prior to Peak Viremia in Acute Human Immunodeficiency Virus Type 1 Infection, in Contrast to More Modest and Delayed Responses in Acute Hepatitis B and C Virus Infections. Journal of Virology. 2009;83(8):3719-33.
9. Altfeld M, Gale M, Jr. Innate immunity against HIV-1 infection. Nat Immunol. 2015;16(6):554-62.
10. Borrow P. Innate immunity in acute HIV-1 infection. Curr Opin HIV AIDS. 2011;6(5):353-63.
11. Borrow P, Lewicki H, Wei X, Horwitz MS, Peffer N, Meyers H, et al. Antiviral pressure exerted by HIV-l-specific cytotoxic T lymphocytes (CTLs) during primary infection demonstrated by rapid selection of CTL escape virus. Nature Medicine. 1997;3(2):205-11.
12. Koup RA, Safrit JT, Cao Y, Andrews CA, McLeod G, Borkowsky W, et al. Temporal association of cellular immune responses with the initial control of viremia in primary human immunodeficiency virus type 1 syndrome. J Virol. 1994;68(7):4650-5.
13. Takata H, Buranapraditkun S, Kessing C, Fletcher JL, Muir R, Tardif V, et al. Delayed differentiation of potent effector CD8(+) T cells reducing viremia and reservoir seeding in acute HIV infection. Sci Transl Med. 2017;9(377).
14. Migueles SA, Sabbaghian MS, Shupert WL, Bettinotti MP, Marincola FM, Martino L, et al. HLA B*5701 is highly associated with restriction of virus replication in a subgroup of HIV-infected long term nonprogressors. Proc Natl Acad Sci U S A. 2000;97(6):2709-14.
15. Einkauf KB, Osborn MR, Gao C, Sun W, Sun X, Lian X, et al. Parallel analysis of transcription, integration, and sequence of single HIV-1 proviruses. Cell. 2022;185(2):266-82.e15.
16. Ho YC, Shan L, Hosmane NN, Wang J, Laskey SB, Rosenbloom DI, et al. Replication-competent noninduced proviruses in the latent reservoir increase barrier to HIV-1 cure. Cell. 2013;155(3):540-51.
17. Migueles SA, Laborico AC, Shupert WL, Sabbaghian MS, Rabin R, Hallahan CW, et al. HIV-specific CD8+ T cell proliferation is coupled to perforin expression and is maintained in nonprogressors. Nat Immunol. 2002;3(11):1061-8.
18. Migueles SA, Osborne CM, Royce C, Compton AA, Joshi RP, Weeks KA, et al. Lytic granule loading of CD8+ T cells is required for HIV-infected cell elimination associated with immune control. Immunity. 2008;29(6):1009-21.

19. Migueles SA, Weeks KA, Nou E, Berkley AM, Rood JE, Osborne CM, et al. Defective human immunodeficiency virus-specific CD8+ T-cell polyfunctionality, proliferation, and cytotoxicity are not restored by antiretroviral therapy. J Virol. 2009;83(22):11876-89.
20. Boppana S, Goepfert P. Understanding the CD8 T-cell response in natural HIV control. F1000Res. 2018;7.
21. van Paassen PM, van Pul L, van der Straten K, Buchholtz NVJE, Grobben M, van Nuenen AC, et al. Virological and immunological correlates of HIV posttreatment control after temporal antiretroviral therapy during acute HIV infection. AIDS. 2023;37(15):2297-304.
22. Blazkova J, Gao F, Marichannegowda MH, Justement JS, Shi V, Whitehead EJ, et al. Distinct mechanisms of long-term virologic control in two HIV-infected individuals after treatment interruption of anti-retroviral therapy. Nature Medicine. 2021;27(11):1893-8.
23. Chowdhury A, Hayes TL, Bosinger SE, Lawson BO, Vanderford T, Schmitz JE, et al. Differential Impact of In Vivo CD8+ T Lymphocyte Depletion in Controller versus Progressor Simian Immunodeficiency Virus-Infected Macaques. J Virol. 2015;89(17):8677-86.
24. McBrien JB, Mavigner M, Franchitti L, Smith SA, White E, Tharp GK, et al. Robust and persistent reactivation of SIV and HIV by N-803 and depletion of CD8(+) cells. Nature. 2020;578(7793):154-9.
25. Passaes C, Desjardins D, Chapel A, Monceaux V, Lemaitre J, Mélard A, et al. Early antiretroviral therapy favors post-treatment SIV control associated with the expansion of enhanced memory CD8+ T-cells. Nature Communications. 2024;15(1):178.
26. Migueles SA, Connors M. Long-term nonprogressive disease among untreated HIV-infected individuals: clinical implications of understanding immune control of HIV. Jama. 2010;304(2):194-201.
27. Betts MR, Nason MC, West SM, De Rosa SC, Migueles SA, Abraham J, et al. HIV nonprogressors preferentially maintain highly functional HIV-specific CD8+ T cells. Blood. 2006;107(12):4781-9.
28. Ndhlovu ZM, Kamya P, Mewalal N, Kløverpris HN, Nkosi T, Pretorius K, et al. Magnitude and Kinetics of CD8+ T Cell Activation during Hyperacute HIV Infection Impact Viral Set Point. Immunity. 2015;43(3):591-604.
29. Ndhlovu ZM, Kazer SW, Nkosi T, Ogunshola F, Muema DM, Anmole G, et al. Augmentation of HIV-specific T cell function by immediate treatment of hyperacute HIV-1 infection. Science Translational Medicine. 2019;11(493):eaau0528.
30. Takata H, Mitchell JL, Pacheco J, Pagliuzza A, Pinyakorn S, Buranapraditkun S, et al. An active HIV reservoir during ART is associated with maintenance of HIV-specific CD8(+) T cell magnitude and short-lived differentiation status. Cell Host Microbe. 2023;31(9):1494-506.e4.
31. Ananworanich J, Chomont N, Eller LA, Kroon E, Tovanabutra S, Bose M, et al. HIV DNA Set Point is Rapidly Established in Acute HIV Infection and Dramatically Reduced by Early ART. EBioMedicine. 2016;11:68-72.
32. Jain V, Hartogensis W, Bacchetti P, Hunt PW, Hatano H, Sinclair E, et al. Antiretroviral therapy initiated within 6 months of HIV infection is associated with lower T-cell activation and smaller HIV reservoir size. J Infect Dis. 2013;208(8):1202-11.
33. Archin NM, Vaidya NK, Kuruc JD, Liberty AL, Wiegand A, Kearney MF, et al. Immediate antiviral therapy appears to restrict resting CD4+ cell HIV-1 infection without accelerating the decay of latent infection. Proc Natl Acad Sci U S A. 2012;109(24):9523-8.
34. Strain MC, Little SJ, Daar ES, Havlir DV, Gunthard HF, Lam RY, et al. Effect of treatment, during primary infection, on establishment and clearance of cellular reservoirs of HIV-1. J Infect Dis. 2005;191(9):1410-8.
35. Ananworanich J, Schuetz A, Vandergeeten C, Sereti I, de Souza M, Rerknimitr R, et al. Impact of Multi-Targeted Antiretroviral Treatment on Gut T Cell Depletion and HIV Reservoir Seeding during Acute HIV Infection. PLOS ONE. 2012;7(3):e33948.
36. Le T, Wright EJ, Smith DM, He W, Catano G, Okulicz JF, et al. Enhanced CD4+ T-Cell Recovery with Earlier HIV-1 Antiretroviral Therapy. New England Journal of Medicine. 2013;368(3):218-30.

607 37. Namazi G, Fajnzylber JM, Aga E, Bosch RJ, Acosta EP, Sharaf R, et al. The Control of HIV After
608 Antiretroviral Medication Pause (CHAMP) Study: Posttreatment Controllers Identified From 14
609 Clinical Studies. J Infect Dis. 2018;218(12):1954-63.
610 38. Bruner KM, Wang Z, Simonetti FR, Bender AM, Kwon KJ, Sengupta S, et al. A quantitative
611 approach for measuring the reservoir of latent HIV-1 proviruses. Nature. 2019;566(7742):120-5.
612 39. Fombellida-Lopez C, Berkhout B, Darcis G, Pasternak AO. Persistent HIV-1 transcription
613 during ART: time to reassess its significance? Curr Opin HIV AIDS. 2024;19(3):124-32.
614 40. Peluso MJ, Bacchetti P, Ritter KD, Beg S, Lai J, Martin JN, et al. Differential decay of intact and
615 defective proviral DNA in HIV-1-infected individuals on suppressive antiretroviral therapy. JCI Insight.
616 2020;5(4).
617 41. Gandhi RT, Cyktor JC, Bosch RJ, Mar H, Laird GM, Martin A, et al. Selective Decay of Intact
618 HIV-1 Proviral DNA on Antiretroviral Therapy. J Infect Dis. 2021;223(2):225-33.
619 42. Nühn MM, Bosman K, Huisman T, Staring WHA, Gharu L, De Jong D, et al. Selective decline of
620 intact HIV reservoirs during the first decade of ART followed by stabilization in memory T cell subsets.
621 Aids. 2025;39(7):798-811.
622 43. Singh K, Natarajan V, Dewar R, Rupert A, Badralmaa Y, Zhai T, et al. Long-term persistence of
623 transcriptionally active 'defective' HIV-1 proviruses: implications for persistent immune activation
624 during antiretroviral therapy. Aids. 2023;37(14):2119-30.
625 44. Imamichi H, Dewar RL, Adelsberger JW, Rehm CA, O'Doherty U, Paxinos EE, et al. Defective
626 HIV-1 proviruses produce novel protein-coding RNA species in HIV-infected patients on combination
627 antiretroviral therapy. Proc Natl Acad Sci U S A. 2016;113(31):8783-8.
628 45. Imamichi H, Smith M, Adelsberger JW, Izumi T, Scrimieri F, Sherman BT, et al. Defective HIV-1
629 proviruses produce viral proteins. Proc Natl Acad Sci U S A. 2020;117(7):3704-10.
630 46. Pollack RA, Jones RB, Pertea M, Bruner KM, Martin AR, Thomas AS, et al. Defective HIV-1
631 Proviruses Are Expressed and Can Be Recognized by Cytotoxic T Lymphocytes, which Shape the
632 Proviral Landscape. Cell Host Microbe. 2017;21(4):494-506.e4.
633 47. Barbehenn A, Shi L, Shao J, Hoh R, Hartig HM, Pae V, et al. Rapid biphasic decay of intact and
634 defective HIV DNA reservoir during acute treated HIV disease. Nature Communications.
635 2024;15(1):9966.
636 48. Reddy K, Lee GQ, Reddy N, Chikowore TJB, Baisley K, Dong KL, et al. Differences in HIV-1
637 reservoir size, landscape characteristics and decay dynamics in acute and chronic treated HIV-1 Clade
638 C infection. medRxiv. 2024:2024.02.16.24302713.
639 49. Massanella M, Ignacio RAB, Lama JR, Pagliuzza A, Dasgupta S, Alfaro R, et al. Long-term
640 effects of early antiretroviral initiation on HIV reservoir markers: a longitudinal analysis of the
641 MERLIN clinical study. Lancet Microbe. 2021;2(5):e198-e209.
642 50. Lian X, Seiger KW, Parsons EM, Gao C, Sun W, Gladkov GT, et al. Progressive transformation
643 of the HIV-1 reservoir cell profile over two decades of antiviral therapy. Cell Host & Microbe.
644 2023;31(1):83-96.e5.
645 51. Jiang C, Lian X, Gao C, Sun X, Einkauf KB, Chevalier JM, et al. Distinct viral reservoirs in
646 individuals with spontaneous control of HIV-1. Nature. 2020;585(7824):261-7.
647 52. Lian X, Gao C, Sun X, Jiang C, Einkauf KB, Seiger KW, et al. Signatures of immune selection in
648 intact and defective proviruses distinguish HIV-1 elite controllers. Science Translational Medicine.
649 2021;13(624):eabl4097.
650 53. Naranbhai V, Carrington M. Host genetic variation and HIV disease: from mapping to
651 mechanism. Immunogenetics. 2017;69(8-9):489-98.
652 54. Gunst JD, Pahus MH, Rosás-Umbert M, Lu IN, Benfield T, Nielsen H, et al. Early intervention
653 with 3BNC117 and romidepsin at antiretroviral treatment initiation in people with HIV-1: a phase
654 1b/2a, randomized trial. Nature Medicine. 2022.
655 55. Dijkstra M, Prins H, Prins JM, Reiss P, Boucher C, Verbon A, et al. Cohort profile: the
656 Netherlands Cohort Study on Acute HIV infection (NOVA), a prospective cohort study of people with
657 acute or early HIV infection who immediately initiate HIV treatment. BMJ Open.
658 2021;11(11):e048582.

659 56. Pasternak AO, Adema KW, Bakker M, Jurriaans S, Berkhout B, Cornelissen M, et al. Highly
660 sensitive methods based on seminested real-time reverse transcription-PCR for quantitation of
661 human immunodeficiency virus type 1 unspliced and multiply spliced RNA and proviral DNA. J Clin
662 Microbiol. 2008;46(7):2206-11.
663 57. Boom R, Sol CJ, Salimans MM, Jansen CL, Wertheim-van Dillen PM, van der Noordaa J. Rapid
664 and simple method for purification of nucleic acids. J Clin Microbiol. 1990;28(3):495-503.
665 58. Malnati MS, Scarlatti G, Gatto F, Salvatori F, Cassina G, Rutigliano T, et al. A universal real-
666 time PCR assay for the quantification of group-M HIV-1 proviral load. Nat Protoc. 2008;3(7):1240-8.
667 59. Bruner KM, Wang Z, Simonetti FR, Bender AM, Kwon KJ, Sengupta S, et al. A quantitative
668 approach for measuring the reservoir of latent HIV-1 proviruses. Nature. 2019;566(7742):120-5.
669 60. Pasternak AO, Jurriaans S, Bakker M, Prins JM, Berkhout B, Lukashov VV. Cellular levels of HIV
670 unspliced RNA from patients on combination antiretroviral therapy with undetectable plasma
671 viremia predict the therapy outcome. PLoS One. 2009;4(12):e8490.
672 61. Fischer M, Huber W, Kallivroussis A, Ott P, Opravil M, Lüthy R, et al. Highly sensitive methods
673 for quantitation of human immunodeficiency virus type 1 RNA from plasma, cells, and tissues. J Clin
674 Microbiol. 1999;37(5):1260-4.
675 62. Levy CN, Hughes SM, Roychoudhury P, Reeves DB, Amstuz C, Zhu H, et al. A highly
676 multiplexed droplet digital PCR assay to measure the intact HIV-1 proviral reservoir. Cell Rep Med.
677 2021;2(4):100243.
678 63. Luo W, Yang H, Rathbun K, Pau CP, Ou CY. Detection of human immunodeficiency virus type
679 1 DNA in dried blood spots by a duplex real-time PCR assay. J Clin Microbiol. 2005;43(4):1851-7.
680 64. van 't Wout AB, Schuitemaker H, Kootstra NA. Isolation and propagation of HIV-1 on
681 peripheral blood mononuclear cells. Nature Protocols. 2008;3(3):363-70.

682

Figure Legends

Figure 1. Correlation matrix of viral reservoir measures at 24 and 156 weeks after start of ART. Correlation coefficients (*rho*) determined by Spearman correlation analyses are shown. Strength of positive and negative correlations is indicated by the color shade displayed in the legend. Significant correlations are indicated by *** if $p<0.001$ or by ** if $p<0.01$. All significant correlations remained significant after corrections for multiple comparisons.

Figure 2. Paired comparisons of viral reservoir measures at 24 and 156 weeks of ART. Open symbols represent values below the detection limits of the assays. The four participants with a positive QVOA at 24 weeks are marked with colors (purple, blue, green, or red). Paired Wilcoxon test was performed to test the significance of the differences between the time points (* if $p<0.05$ or ** if $p<0.01$). Pairs where both values were undetectable, or where one was undetectable and its detection limit was higher than the value of the detectable partner, were excluded from the analysis. Exact p values are indicated below the graphs.

Figure 3. Correlations of reservoir measures and HIV-specific CD8+ T-cell responses as determined by IFN-γ release assay, AIM, and proliferation assay (proliferating cells and precursor cells). The immune responses are defined as the sum of the responses to Env, Gag, Nef and Pol combined at 24 and 156 weeks. Correlation coefficients (*rho*) determined by Spearman correlation analyses are shown. Strength of positive and negative correlations is indicated by the color shade displayed in the legend. Significant correlations are indicated by *** if $p<0.001$ or by ** if $p<0.01$. All significant correlations remained significant after corrections for multiple comparisons.

Suppl. Fig. 1. Overview of NOVA cohort study procedures for study groups 2 and 3. ART, combination antiretroviral therapy; GALT, gut-associated lymphoid tissue; PBMC, peripheral

blood mononuclear cells. Retrieved from: *Dijkstra M. et al. Cohort profile: the Netherlands Cohort Study on Acute HIV infection (NOVA), a prospective cohort study of people with acute or early HIV infection who immediately initiate HIV treatment. BMJ Open. 2021;11(11):e048582.*

Suppl. Fig. 2. A. Plasma viral load (pVL) B. CD4 T-cell count (x10^6/mL) and C. CD4/CD8 ratio at baseline, 24 weeks and 156 weeks post ART initiation. Participant X (green dot) had detectable loads of 200 and 100 cp/mL at 24 and 156 weeks. Participant Y (pink dot) had detectable loads of 74 and 98 cp/mL at 24 and 156 weeks. Lower limit of quantification of the assays used ranged between 40 copies (earlier) and 20 copies (later time points) (see Methods).

Suppl. Figure 3. Comparison of intact HIV DNA levels at 24 weeks ART between participants with positive (n=6) and negative (n=14) QVOA. Mann-Whitney test was used to determine statistical significance. *, $0.01<p<0.05$.

Suppl. Figure 4. Longitudinal analysis of frequencies of activated and naive, memory and effector subsets within the CD4+ (A) and CD8+ T-cell (B) populations. Wilcoxon signed rank test ($p<0.05$) was used to determine statistical significance of the differences between the timepoints.

Suppl. Figure 5. A. The frequency of dextramer+ CD8+ T-cells at 24 and 156 weeks after ART. B. The expression of exhaustion markers (upregulation of PD-1, CTLA-4, and CD160 expression; loss of CD28 expression) on HIV-dextramer specific CD8+ T-cells at 24 and 156 weeks after ART. For participants that were HLA-A*2 and HLA-B*7 positive, HLA-A*2 and HLA-B*7 dextramer staining was included separately. HLA-A*2 dextramer is marked as a triangle and HLA-B*7 dextramer as a square in both figures.

Suppl. Fig. 6. HIV-specific T-cell responses upon HIV-peptide stimulation (Env, Gag, Nef, Pol) at 24 and 156 weeks after ART: IGRA/ IFN-γ release (A), AIM reactive CD8+ T-cells (B),

precursor frequency (C) and the proportion of proliferating CD8+ T-cells (D). Frequencies of proliferating cells in response to Env, Gag, Nef and Pol peptides were combined. Overall, no significant difference in IGRA over time was observed.

Suppl. Figure 7. Correlation matrix of reservoir measurements and the frequency of dextramer+ CD8+ T-cell responses at 24 and 156 weeks after ART initiation. The correlation coefficient (*rho*) determined by Spearman correlation is shown. Positive and negative correlations (*rho*) are indicated by the color shade displayed in the legend. Significant correlations are indicated by * if $p<0.05$ or ** if $p<0.01$.

Table 1. Characteristics of the study participants.

		Total (n=22)	Paired analysis (n=12)[a]
Sex at birth, male		100%	
Age at inclusion, years[b]		38 (28 – 48)	40.5 (25.5 – 49)
Country of birth	The Netherlands	18	12
	Other	4	0
Fiebig stage at diagnosis[c]	II	1	0
	III – IV	12	7
	V	5	4
	VI	4	1
Plasma viral load at baseline, 10^6 copies/mL		0.4 (0.04 – 10)	0.61 (0.28 – 10)
CD4+ T-cell count at baseline, cells/mm^3		445 (308-593)	435 (295 – 555)
HIV subtype	B	15	10
	CRF02_AG	1	0
	AE	3	1
	F	2	1
	Unknown	1	0
Time between diagnosis and start of ART	Same day	15	8
	1 day	3	1
	2 days	2	1
	Unknown	2	2

[a] Participants with available samples from both 24-week and 156-week time points.
[b] Medians and interquartile ranges are shown for continuous variables.
[c] Fiebig, E. W. et al. Dynamics of HIV viremia and antibody seroconversion in plasma donors: implications for diagnosis and staging of primary HIV infection. AIDS 17, 1871–1879 (2003).

Table 2. Variables measured at 24 weeks ART associated with the changes in HIV-1 reservoir markers between 24 and 156 weeks of ART.

Variable	Total HIV-1 DNA[a]		Intact HIV-1 DNA		Defective HIV-1 DNA	
	Effect size (95% CI)	p[b]	Effect size (95% CI)	p	Effect size (95% CI)	p
Age, per year	-2.99 (-28.5 – 22.5)	0.60	-0.49 (-5.00 – 4.02)	0.86	1.19 (-14.3 – 16.7)	0.66
NRTI backbone, ABC+3TC vs. FTC+TDF/TAF[c]	-1.10 (-4.80 – 2.60)	0.56	-0.67 (-4.56 – 3.22)	0.74	2.67 (-0.94 – 6.27)	0.15
IFN-γ release, per pg/ml	2.40 (-13.2 – 18.0)	0.79	-1.32 (-4.04 – 1.40)	0.59	-5.29 (-14.4 – 3.81)	0.14
CD8+ T-cell reactivity, per %	-537 (-1677 – 603)	0.27	-85.6 (-298 – 127)	0.25	-361 (-1073 – 351)	0.15
CD8+ T-cell proliferation, per %	62.7 (28.7 – 96.7)	0.014	2.84 (-4.62 – 10.3)	0.56	37.8 (18.5 – 57.1)	0.0017

[a] Total, intact, and defective HIV-1 DNA are in copies/10^6 PBMC.
[b] Calculated by fitting generalized linear models (GLM), type III tests were used.
[c] Six participants were treated with ABC+3TC and six participants – with FTC+TDF or FTC+TAF as an NRTI backbone.

Figure 1

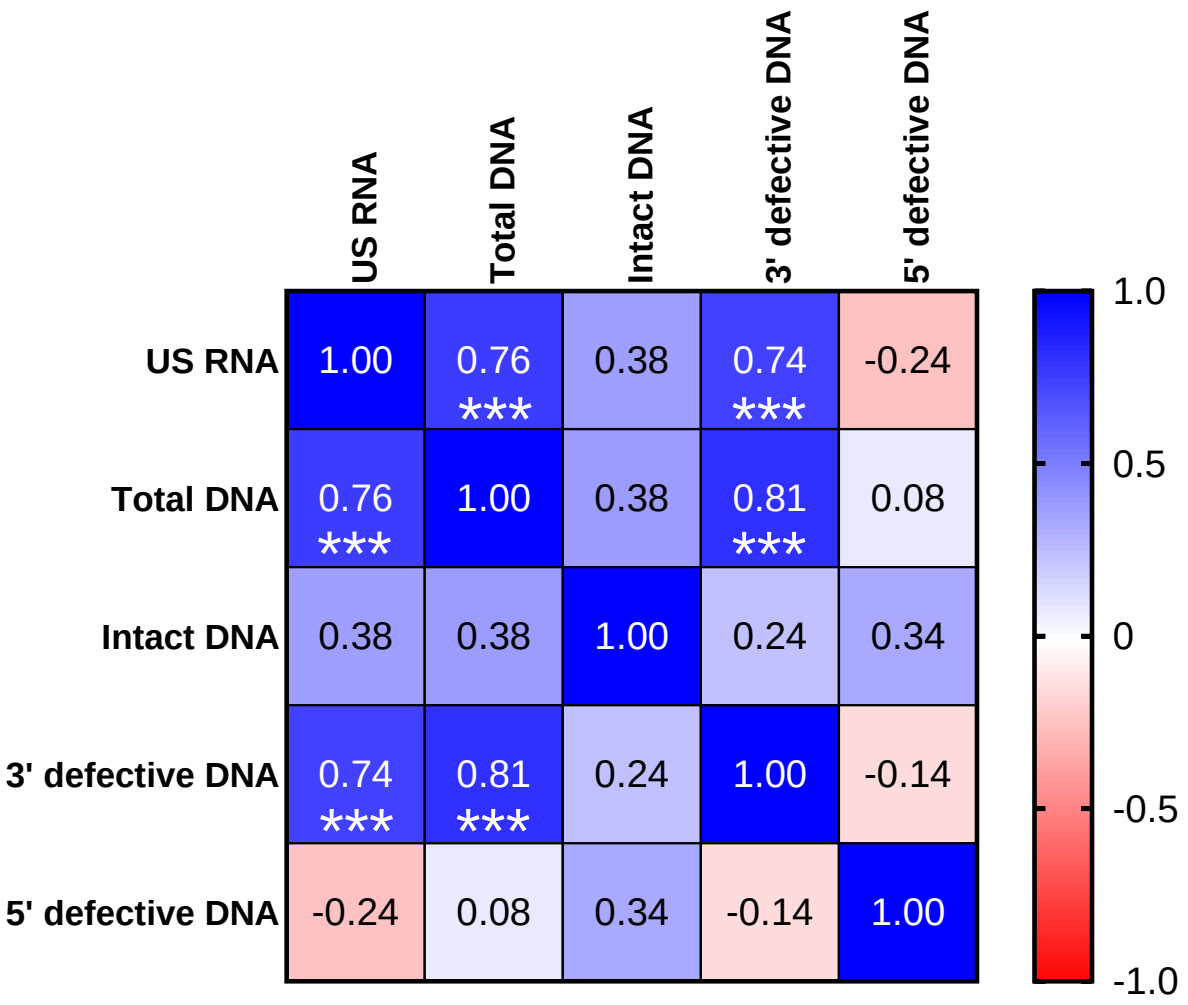

24 weeks

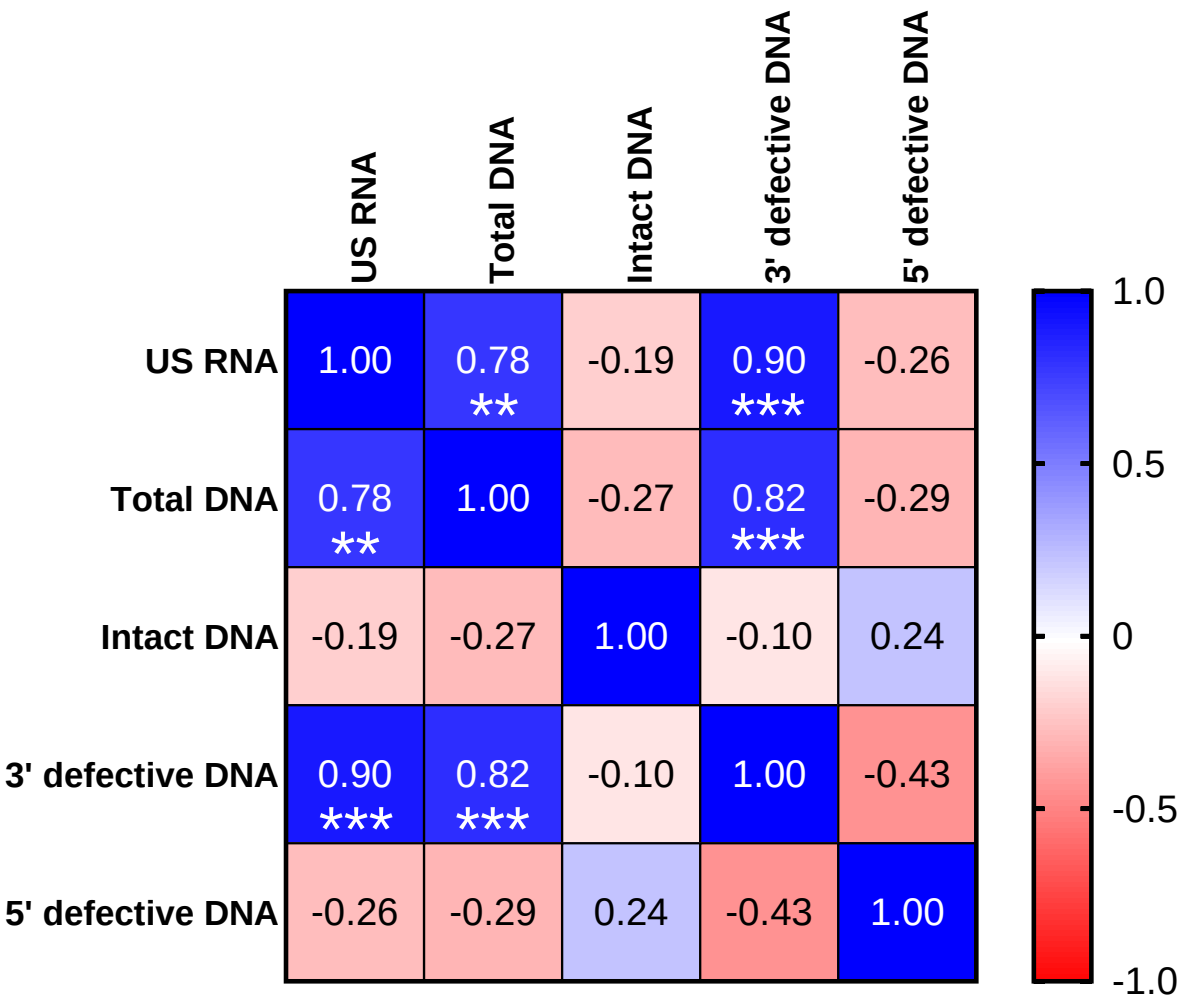

156 weeks

Figure 2

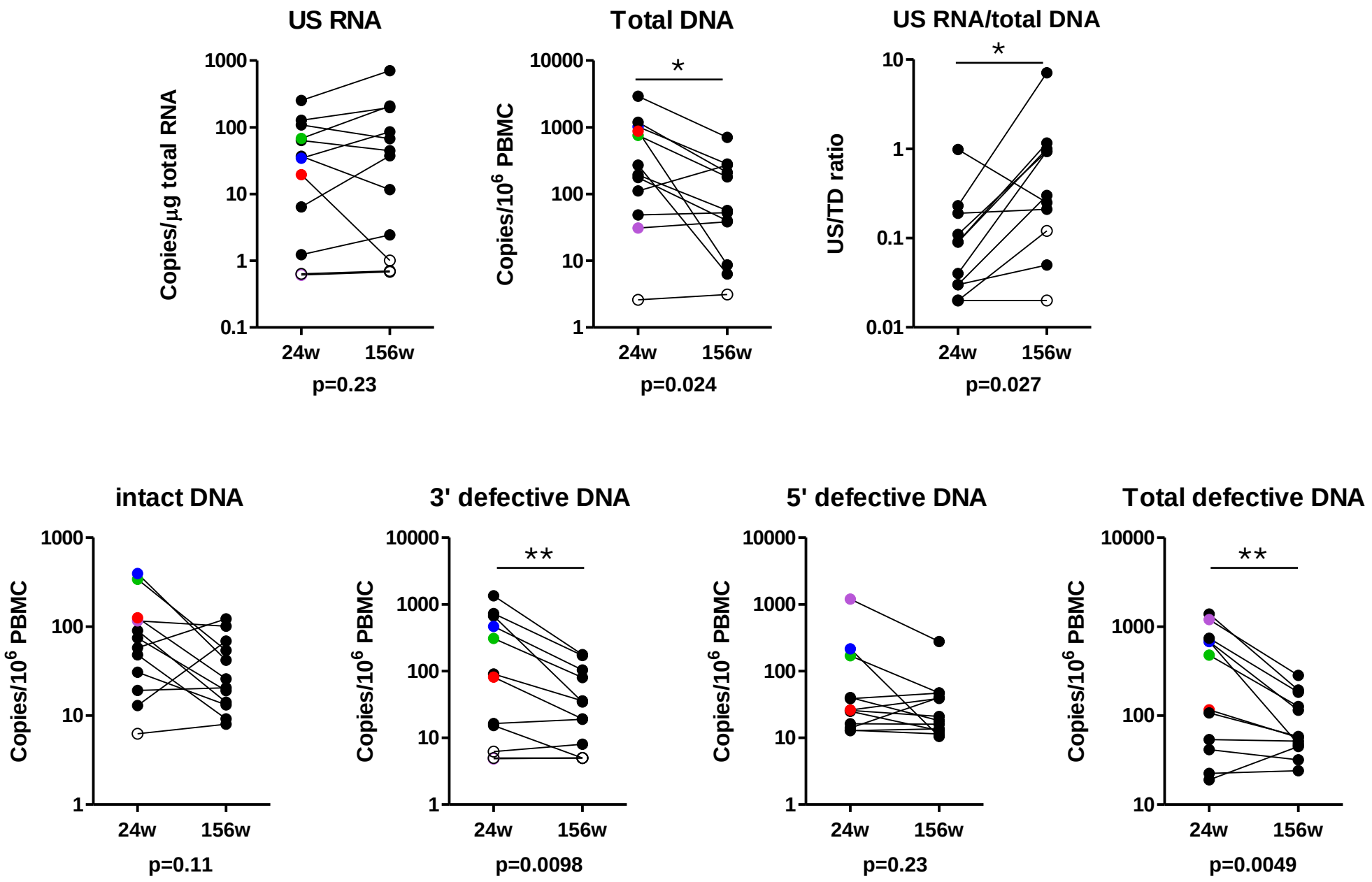
US RNA
Copies/μg total RNA
1000
100
10
1
0.1
24w
156w
p=0.23
Total DNA
Copies/10^6 PBMC
10000
1000
100
10
1
*
24w
156w
p=0.024
US RNA/total DNA
US/TD ratio
10
1
0.1
0.01
*
24w
156w
p=0.027
intact DNA
Copies/10^6 PBMC
1000
100
10
1
24w
156w
p=0.11
3' defective DNA
Copies/10^6 PBMC
10000
1000
100
10
1
**
24w
156w
p=0.0098
5' defective DNA
Copies/10^6 PBMC
10000
1000
100
10
1
24w
156w
p=0.23
Total defective DNA
Copies/10^6 PBMC
10000
1000
100
10
**
24w
156w
p=0.0049

Figure 3

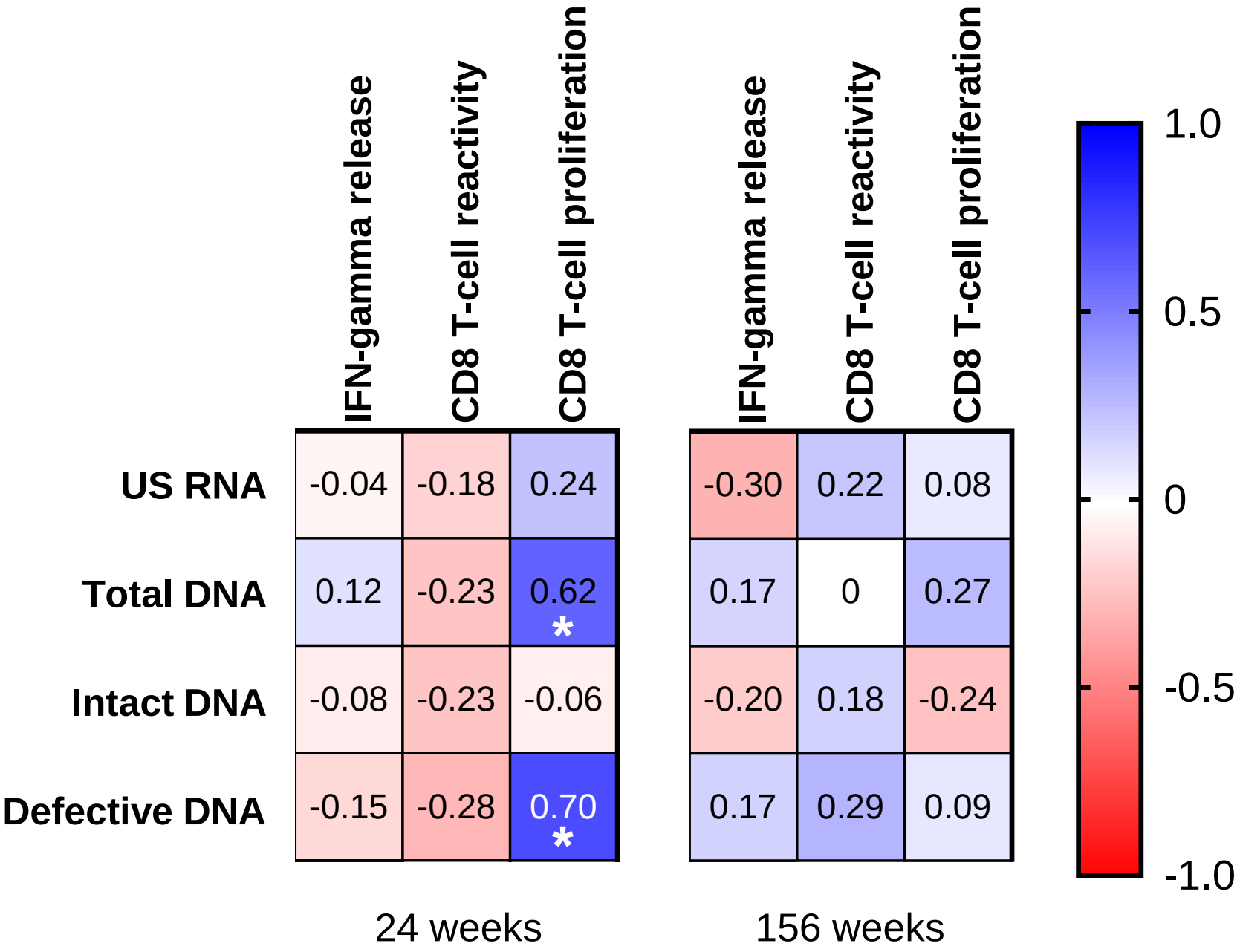
IFN-gamma release
CD8 T-cell reactivity
CD8 T-cell proliferation
IFN-gamma release
CD8 T-cell reactivity
CD8 T-cell proliferation
US RNA
Total DNA
Intact DNA
Defective DNA
-0.04
-0.18
0.24
0.12
-0.23
0.62
*
-0.08
-0.23
-0.06
-0.15
-0.28
0.70
*
-0.30
0.22
0.08
0.17
0
0.27
-0.20
0.18
-0.24
0.17
0.29
0.09
24 weeks
156 weeks
1.0
0.5
0
-0.5
-1.0

Supplementary Figures

Supp. Fig. 1

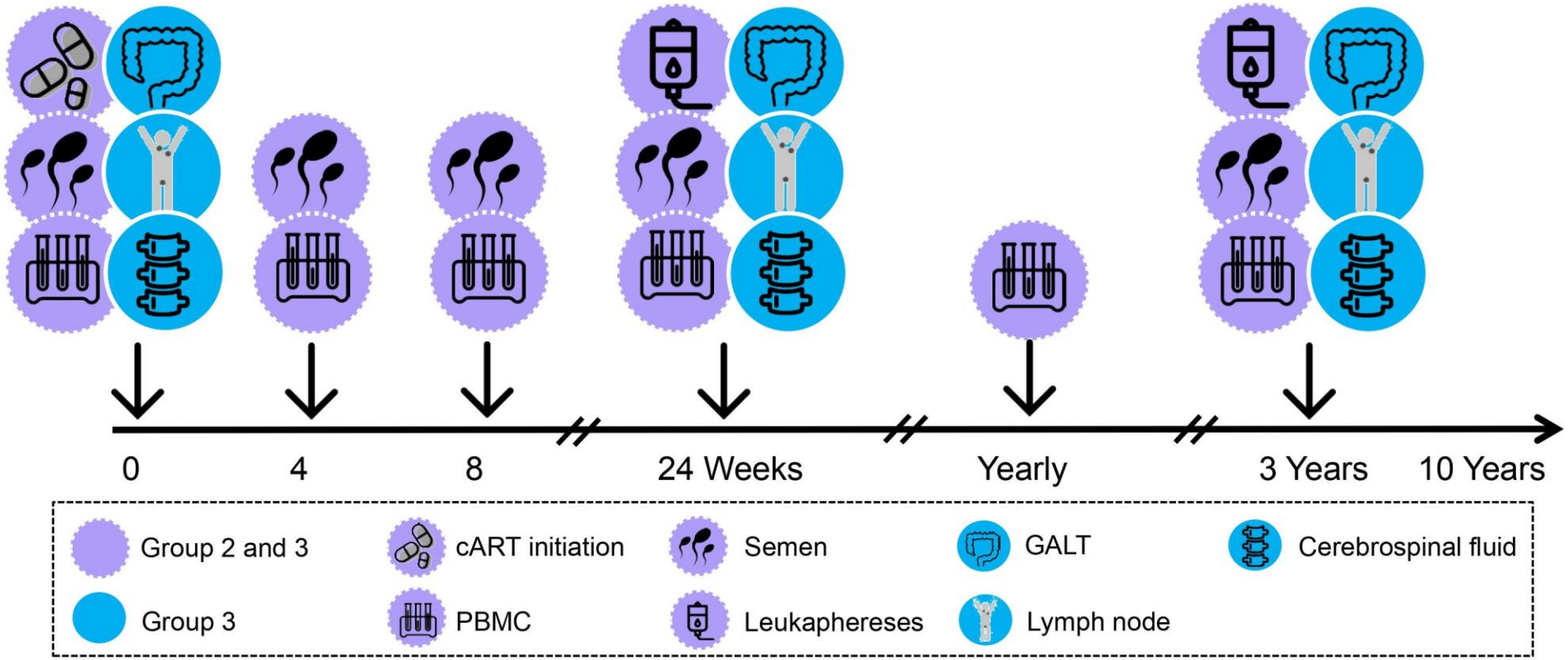
0
4
8
24 Weeks
Yearly
3 Years
10 Years
Group 2 and 3
Group 3
cART initiation
PBMC
Semen
Leukaphereses
GALT
Lymph node
Cerebrospinal fluid

Suppl. Fig. 2

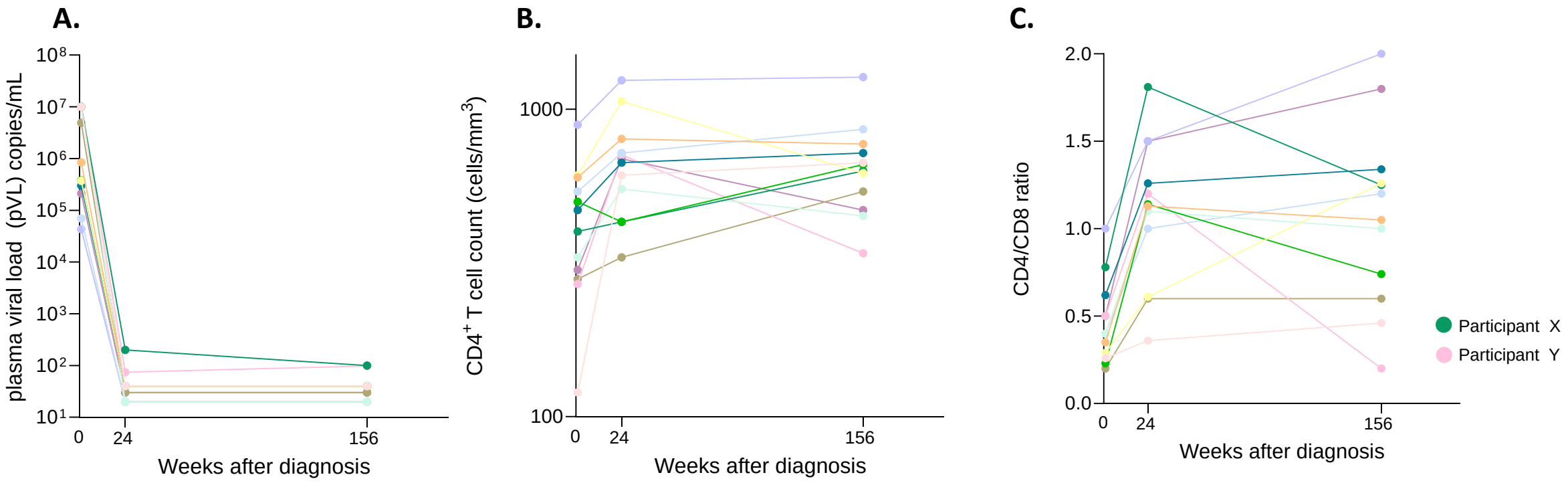
A.
plasma viral load (pVL) copies/mL
10^8
10^7
10^6
10^5
10^4
10^3
10^2
10^1
0
24
156
Weeks after diagnosis
B.
$CD4^+$ T cell count (cells/mm^3)
1000
100
0
24
156
Weeks after diagnosis
C.
CD4/CD8 ratio
2.0
1.5
1.0
0.5
0.0
0
24
156
Weeks after diagnosis
Participant X
Participant Y

Suppl. Fig. 3

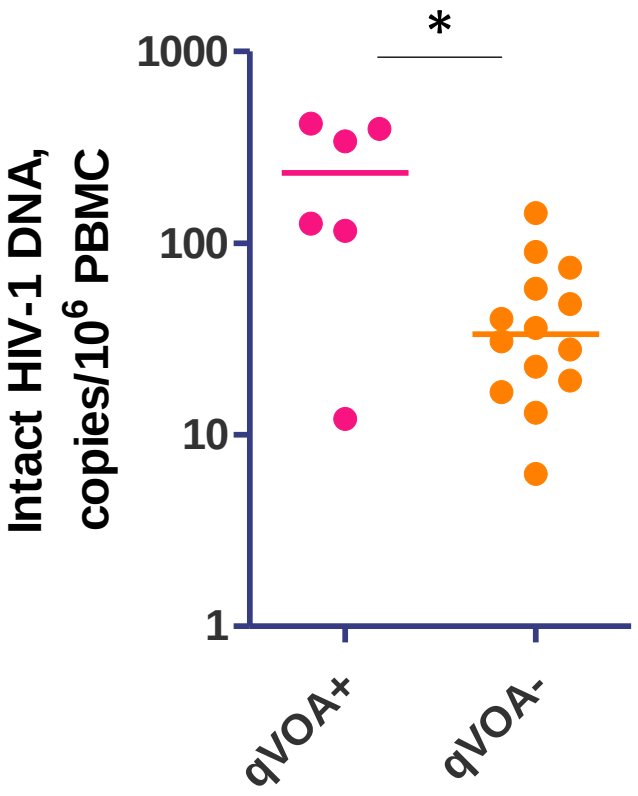

Suppl. Fig. 4

A.

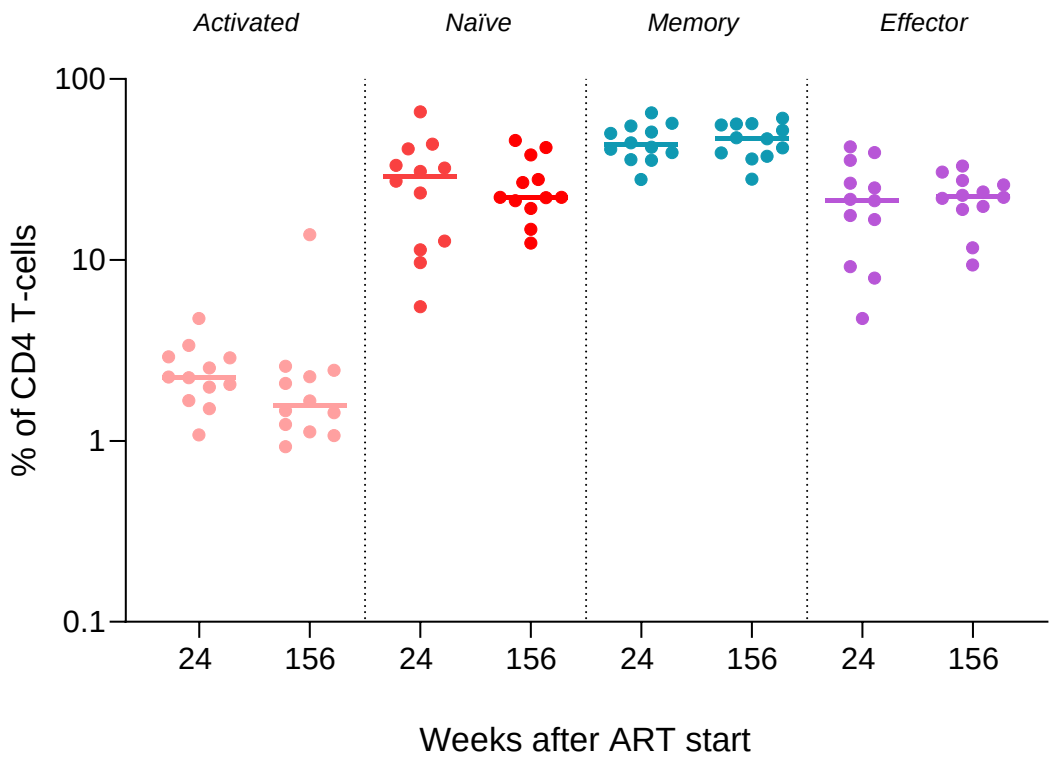

B.

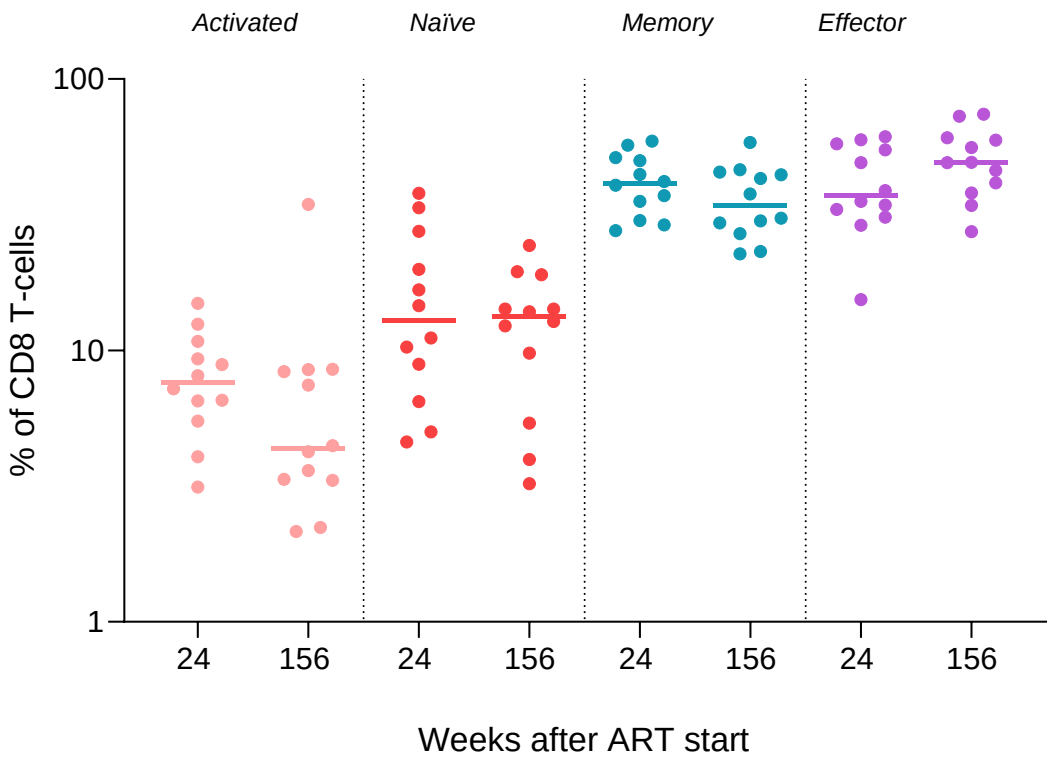

Suppl. Fig. 5

A.

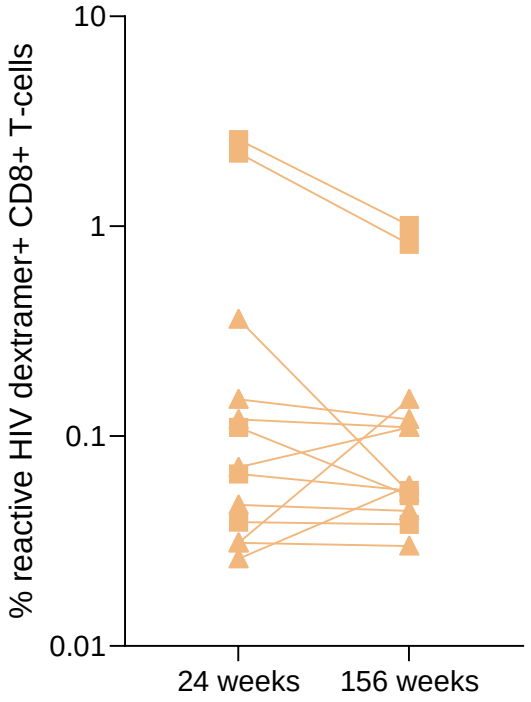

B.

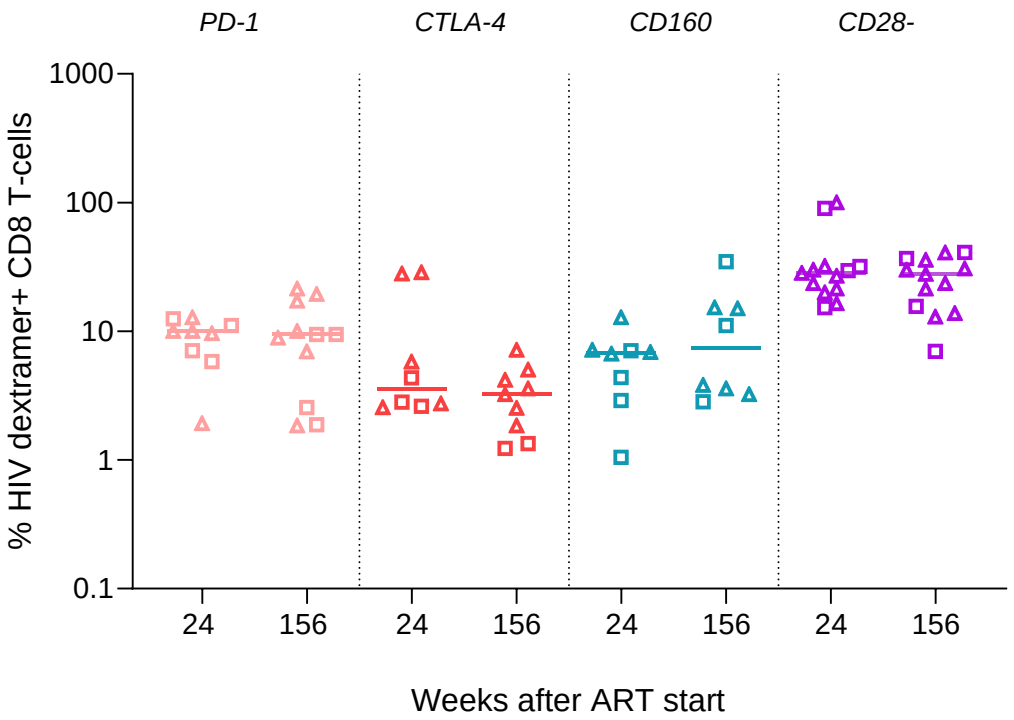

Suppl. Fig. 6

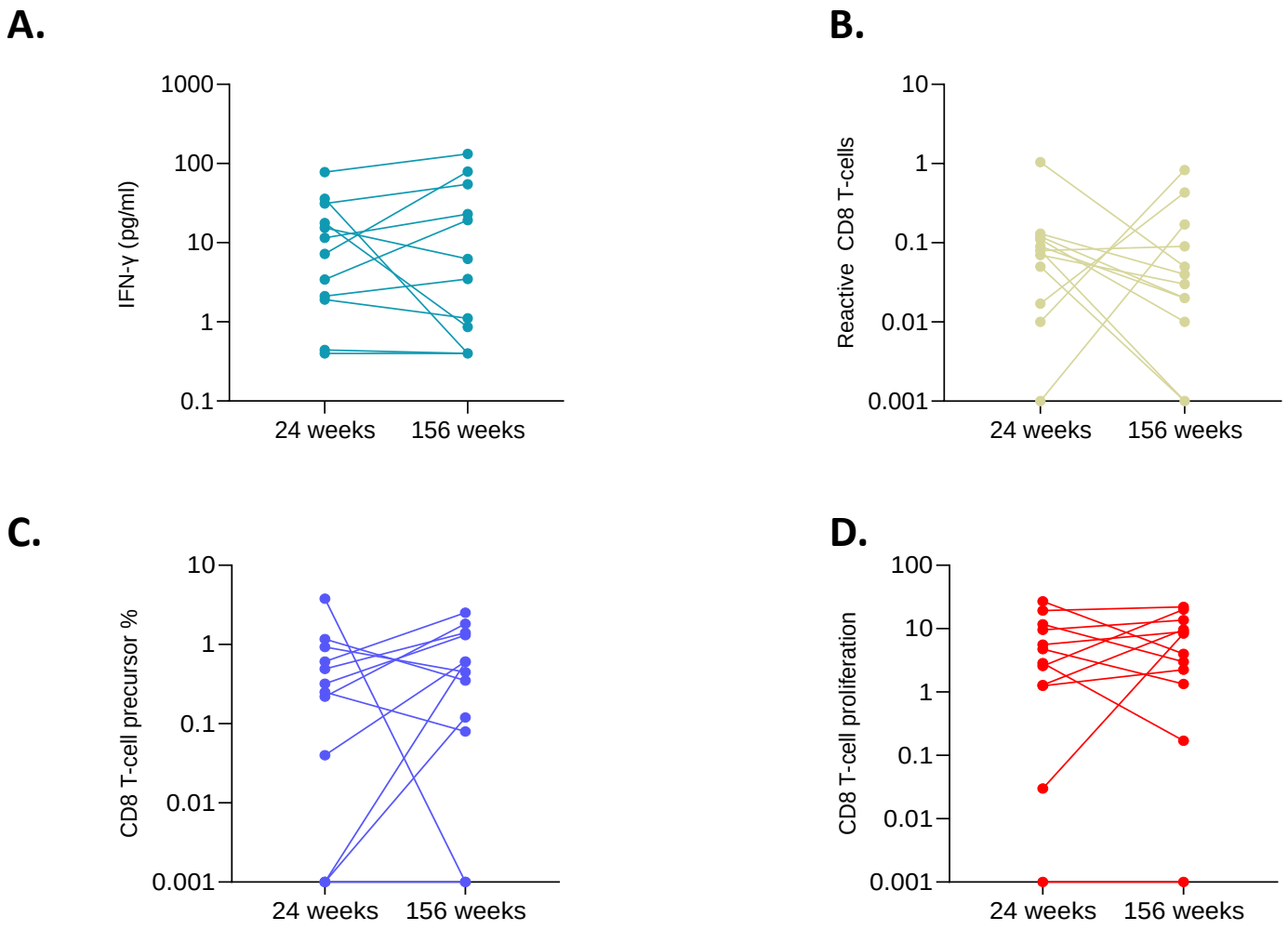
A.
IFN-γ (pg/ml)
1000
100
10
1
0.1
24 weeks
156 weeks
B.
Reactive CD8 T-cells
10
1
0.1
0.01
0.001
24 weeks
156 weeks
C.
CD8 T-cell precursor %
10
1
0.1
0.01
0.001
24 weeks
156 weeks
D.
CD8 T-cell proliferation
100
10
1
0.1
0.01
0.001
24 weeks
156 weeks

Suppl. Fig. 7

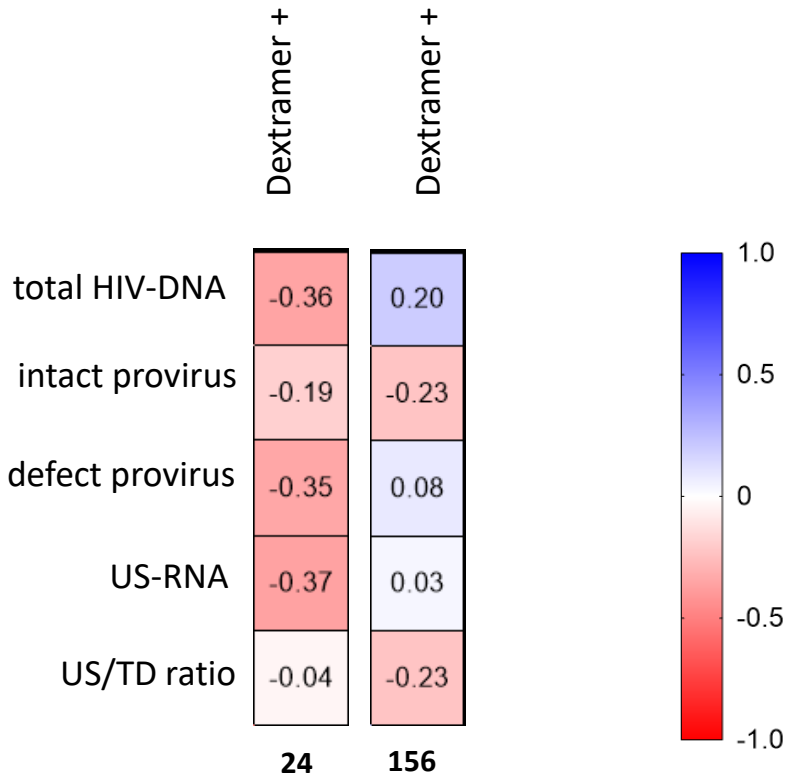
Dextramer +
Dextramer +
total HIV-DNA
intact provirus
defect provirus
US-RNA
US/TD ratio
-0.36
0.20
-0.19
-0.23
-0.35
0.08
-0.37
0.03
-0.04
-0.23
24
156
1.0
0.5
0
-0.5
-1.0